HOKKAIDO UNIVERSITY

Title	Correction of sonic anemometer angle of attack errors
Author(s)	Nakai, Taro; van der Molen, M.K.; Gash, J.H.C. et al.
Citation	Agricultural and Forest Meteorology, 136(1-2), 19-30 https://doi.org/10.1016/j.agrformet.2006.01.006
Issue Date	2006-01-11
Doc URL	https://hdl.handle.net/2115/34770
Type	journal article
File Information	Nakai_2006AFM_HUSCAP.pdf

Hokkaido University Collection of Scholarly and Academic Papers : HUSCAP

Correction of sonic anemometer angle of attack errors

Taro Nakai [a,b,*], M.K. van der Molen [c,1], J.H.C. Gash [d,2], Yuji Kodama [b,3]

[a] *CREST, Japan Science and Technology Agency, Kawaguchi, Saitama 332-0012, Japan*

[b] *Institute of Low Temperature Science, Hokkaido University, N19 W8, Kita-Ku, Sapporo 060-0819, Japan*

[c] *Department of Hydrology and Geo-Environmental Sciences, Faculty of Earth and Life Sciences, Vrije Universiteit, de Boelelaan 1085, 1081 HV, Amsterdam, The Netherlands*

[d] *Centre for Ecology and Hydrology, Wallingford OX10 8BB, UK*

Abstract

An improved method of correcting for the angle of attack error resulting from the imperfect (co)sine response of ultrasonic anemometers is proposed. The angle of attack, which was calculated as the arctangent of observed wind vectors, contains the angle of attack errors in the vectors themselves, and hence this angle was 'false'. The 'true' angle of attack should be calculated from the corrected or 'true' wind vectors. In the improved method, the 'true' angle of attack is derived by solving a nonlinear equation which connects the 'false' angle of attack to the 'true' one. In applying this method to the case of R2- and R3-type Solent ultrasonic anemometers, the fit of the function for the sine responses to wind tunnel data was improved, and

the cosine response function was also improved to consider the effect of the difference of the vertical positions of the transducers. The nonlinear equation was solved using the Steffensen method; robustly and adequately fast for practical use in calculating eddy fluxes. The accuracy of the correction method is improved over a previous one, especially at large angles of attack. Applying our correction method to field data from two forests and one peat bog, the eddy fluxes of sensible heat, latent heat and CO_2 were increased and the energy balance closure rates were improved. These results indicate that a large portion of energy imbalance can be accounted for by the ultrasonic anemometer angle of attack dependent errors.

Key words: angle of attack, ultrasonic anemometer, eddy covariance, nonlinear equation

1 Introduction

Angle of attack error results from the imperfect (co)sine response of anemometers. When the instantaneous wind vector is non-horizontal, but has an angle of attack, α (deg), to the horizontal plane, the measured wind may differ substantially from the true value. For ultrasonic anemometers, the effect is the result of self-sheltering by the transducers or flow distortion induced by the frame of the anemometer. The error is likely to increase with angle of attack

* Corresponding author. Tel.: +81-11-706-7437; fax: +81-11-706-7142.
Email addresses: taro@pop.lowtem.hokudai.ac.jp (Taro Nakai), michiel.van.der.molen@falw.vu.nl (M.K. van der Molen), jhg@ceh.ac.uk (J.H.C. Gash), kod@pop.lowtem.hokudai.ac.jp (Yuji Kodama).
[1] Fax: +31-20-598-9940
[2] Fax: +44-1491-692338
[3] Fax: +81-11-706-5509

(see Kaimal and Finnigan, 1994).

Gash and Dolman (2003) examined the potential impact of the instantaneous angle of attack calculated for each sample of two sets of flux measurements made using Solent R3-50 and Windmaster Pro (Gill Instruments, Lymington, UK) anemometers. The manufacturer of these instruments recommends an angle of attack operating envelope of $\pm 20^{\circ}$. However by calculating the flux-angle distribution, Gash and Dolman (2003) found that a large proportion of daytime fluxes (about 20% over short vegetation and about 50% over forest) were carried by eddies with the angles of attack outside this limit, even though the frequencies of occurrence of these angles were relatively low. They also showed the standard deviation of the angle of attack depended on surface roughness, measurement height and atmospheric stability. These results were consistent with previous observations that energy balance closure was worse over forest than over short vegetation (Wilson et al., 2002), and led to the conclusion that angle of attack dependent error was a likely equipment-related cause of the energy balance closure problem.

The error can be removed by using a non-linear, angle of attack dependent calibration, which must be expected to vary with the size and shape of the anemometer. Hence a calibration for each model of anemometer needs to be derived by wind tunnel experiment. Van der Molen et al. (2004) conducted wind tunnel experiments on the R2- and R3-type Solent ultrasonic anemometers (Gill Instruments, Lymington, UK). They showed that the normalised vertical velocity against angles of attack deviated from the ideal sine response considerably, particularly at large angles of attack. The error increased from about 2% at zero angle to about 15% at $\alpha = \pm 60^{\circ}$, and up to 60% at $\alpha = \pm 90^{\circ}$. They also showed that the normalized horizontal velocity against angles of at-

tack was underestimated for positive angles of attack α (updraughts) and overestimated for negative α (downdraughts) compared with the ideal cosine response in the wind direction $0° \leq \gamma \leq 60°$. This behaviour depended on the wind direction γ and was the largest at $\gamma = 30°$ where the wind blows directly on to the lower transducer.

From the results of the wind tunnel experiment, van der Molen et al. (2004) fitted functions to give the measured (co)sine responses as a function of the angle of attack, α and wind direction, γ, and proposed a method to calibrate the vertical and horizontal wind components. Applying this method to field data, van der Molen et al. (2004) showed that introducing the angle of attack dependent calibration changed the calculated fluxes between -5 and $+15\%$, thus generally giving a worthwhile improvement in the energy balance closure.

However, their method had some uncertain points. First, as mentioned by van der Molen et al. (2004), the 'true' angle of attack α cannot be derived from the arctangent of the observed horizontal windspeed U (m s^{-1}) and vertical windspeed w (m s^{-1}), because these measured values are themselves subject to the angle of attack error, as shown in Fig. 1. The 'true' angle of attack must be calculated from the 'corrected' windspeeds, U_c (m s^{-1}) and w_c (m s^{-1}). To avoid this problem, van der Molen et al. (2004) calculated U_c and w_c using the following iterative procedure.

(1) Assuming α as $\alpha = \alpha' = \arctan(w/U)$ (where α' is the 'false', or measured, angle of attack) provides a first estimate of the angle of attack, from the observed vertical and horizontal windspeed components w and U, that are subject to the (co)sine response errors.
(2) Apply α (and the wind direction γ) in the angle of attack dependent

calibration:

$$w_c = w \frac{\sin\alpha}{\sin\alpha + \varepsilon_{\sin}} \tag{1}$$

$$U_c = U \frac{\cos\alpha}{\cos\left(f(\alpha,\gamma)\right)} \tag{2}$$

where $\varepsilon_{\sin}$ and $f(\alpha,\gamma)$ are as defined by van der Molen et al. (2004).

(3) With the calibrated w_c and U_c, an improved estimate of the angle of attack can be obtained: $\alpha = \arctan(w_c/U_c)$.

(4) If this improved α is now applied in step (2), while still using the observed, uncorrected w and U, Eqs. (1) and (2) will yield subsequently better estimates of the calibrated w_c and U_c.

Van der Molen et al. (2004) noted that this procedure may be performed with a number of iterations, but with more than two iterations the extra accuracy proves smaller than the measurement accuracy of the wind tunnel data. However, although time consuming complication should be avoided if it does not affect the final result, best practise would be to obtain the most accurate and efficient method of calculation. From this point of view, there is still uncertainty whether α in Step (3) is equal to the 'true' angle of attack.

Second, w_c from equation (1) diverges at about $\alpha = -0.64°$ because $\sin\alpha + \varepsilon_{\sin} \rightarrow 0$. This leads $|\alpha|$ to be calculated as a large value in Step (3), and hence $|w_c|$ is overestimated and U_c is underestimated in the subsequent iterative calculation.

The best way to solve the above problems would be to derive the 'true' angle of attack α. In this study, we propose an improved, practical method to correct the ultrasonic anemometer angle of attack errors by deriving the 'true' angle of attack, and apply this method to the actual field eddy covariance data.

The van der Molen et al. (2004) wind tunnel data have also been used in this study.

2 Methods

2.1 New method for correction of angle of attack errors

From the results of wind tunnel experiments of van der Molen et al. (2004), the corrected w_c and U_c are written as follows.

$$w_c = w\frac{\sin\alpha}{f_{\mathrm{sr}}(\alpha)} \tag{3}$$

$$U_c = U\frac{\cos\alpha}{f_{\mathrm{cr}}(\alpha,\gamma)} \tag{4}$$

where $f_{\mathrm{sr}}(\alpha)$ and $f_{\mathrm{cr}}(\alpha,\gamma)$ are functions fitted to the actual data of sine response and cosine response, respectively. From these relationships, the nonlinear equation for α is derived as follows.

$$\frac{w}{U}(=\tan\alpha') = \frac{f_{\mathrm{sr}}(\alpha)}{f_{\mathrm{cr}}(\alpha,\gamma)} \tag{5}$$

Since w, U and γ are known, Eq. (5) gives an analytical estimate of α. In calculating this equation, we adopted the Steffensen method (Johnson et al., 1968; Farnum, 1991; Bruden and Fairs, 2004), which is an acceleration method for solving a nonlinear equation. The actual method of calculation is noted in Appendix A.

From the obtained 'true' angle of attack α, observed w and U are corrected to w_c and U_c by Eqs. (3) and (4), respectively. However, w_c from Eq. (3) can diverge at the angle where $f_{\mathrm{sr}}(\alpha) = 0$, and hence w_c is recommended to be

calculated as

$$w_c = U_c \tan \alpha \tag{6}$$

after calculating U_c. Note that for the case when $u = v = 0$, w_c should be calculated from Eq. (3) because $U_c = 0$ and $\tan \alpha = \infty$.

Overall the correction method can be summarised as follows. Once the nonlinear equation is determined from the fitted functions $f_{\mathrm{sr}}(\alpha)$ and $f_{\mathrm{cr}}(\alpha, \gamma)$ with Eq. (5), the correction for ultrasonic anemometer angle of attack errors can be made using the following procedure.

(1) Input observed 3 dimensional wind components u, v and w, and calculate $U = \sqrt{u^2 + v^2}$ and wind direction γ from u and v.
(2) Solve the nonlinear equation using Steffensen method and derive 'true' angle of attack α.
(3) Calculate u_c and v_c from Eq. (4) substituting u, v for U.
(4) Calculate w_c from Eqs. (3) or (6) where $U_c = \sqrt{u_c^2 + v_c^2}$.

This process must be applied to each individual raw measurement of u, v and w before any other calculation or correction procedure used in calculating eddy fluxes.

2.2 Application to the case of R2- and R3-type Solent ultrasonic anemometer

2.2.1 Sine response

The sine response function $f_{\mathrm{sr}}(\alpha)$ used by van der Molen et al. (2004) had two problems. Firstly there is a discontinuity at $\alpha = 0°$ because $f_{\mathrm{sr}}(0)$ is different

when approached from the positive and negative sides. This discontinuity may lead to an endless loop in applying the nonlinear equation for small α. Secondly $f_{\rm sr}(\alpha)$ does not fit well at large angles of attack, $|\alpha| > 80°$.

From the wind tunnel experiment, the actual sine response $a_{\rm sr}(\alpha)$ had the offset $a_{\rm sr}(0)$ at $\alpha = 0°$, and when $a_{\rm sr}(0)$ was subtracted from $a_{\rm sr}(\alpha)$, then $a_{\rm sr}(\alpha) - a_{\rm sr}(0)$ had the same sign with $\sin\alpha$. Considering the characteristics of $(a_{\rm sr}(\alpha) - a_{\rm sr}(0))/\sin\alpha$, we found it had the shape of logistic curve shown in Fig. 2. Following van der Molen et al. (2004), we assume the effect is independent of windspeed and best given by averaging the more accurate, higher windspeed conditions at 8 and 16 m s^{-1}. Hence, we propose the alternative function for fitting to the averaged data of 8 and 16 m s^{-1} (circles in Fig. 2) with logistic regression.

$$f_{\rm sr}(\alpha) = L(\alpha)\sin\alpha + a_{\rm sr}(0) \tag{7}$$

where $a_{\rm sr}(0) = 0.0195$ and $L(\alpha)$ is the logistic regression function estimated by using Marquardt's method (Conway et al., 1970) and given as follows.

$$L(\alpha) = \frac{p_1}{1 + p_2\exp(-p_3(\alpha + 90))} + p_4 \qquad (-90 \le \alpha < 0) \tag{8}$$

$$L(\alpha) = -\frac{p_1}{1 + p_2\exp(-p_3\alpha)} + p_4 \qquad (0 \le \alpha \le 90) \tag{9}$$

The coefficients p_1, p_2, p_3 and p_4 are tabulated in Table 1. Though $L(\alpha)$ is a step function and has a discontinuity at $\alpha = 0°$ (Fig. 2), $\sin\alpha = 0$ at $\alpha = 0°$ and hence Eq.(7) is continuous.

Figure 3 is the result of the new sine response function $f_{\rm sr}(\alpha)$. The circles indicate the observed $a_{\rm sr}(\alpha)$ averaged for the windspeeds 8 and 16 m s^{-1}, and the errorbars show the maximum and minimum values of all the observed

$a_{\mathrm{sr}}(\alpha)$ at each angle of attack α. Figure 3 shows that $f_{\mathrm{sr}}(\alpha)$ gives a good fit to all the observed data, even at large angle of attack $|\alpha| > 80°$. The root mean square error (RMSE) of $f_{\mathrm{sr}}(\alpha)$ was 0.0083 which is an improvement over that given by van der Molen et al. (2004) (RMSE= 0.0268). Furthermore, this function is continuous for $\alpha = 0$ ($f_{\mathrm{sr}}(0) = a_{\mathrm{sr}}(0) = 0.0195$).

2.2.2 Cosine response

Van der Molen et al. (2004) regarded the behaviour of the observed cosine response $a_{\mathrm{cr}}(\alpha, \gamma)$ as the phase shifted cosine function, and proposed the following cosine response function $f_{\mathrm{cr}}(\alpha, \gamma)$.

$$f_{\mathrm{cr}}(\alpha, \gamma) = \cos\left(f(\alpha, \gamma)\right). \tag{10}$$

The angle function $f(\alpha, \gamma)$ (deg) is the polynomial of α and written as follows:

$$f(\alpha, \gamma) = q_1\alpha^3 + q_2\alpha^2 + q_3\alpha + \delta(\gamma), \tag{11}$$

where $\delta(\gamma)$ is the wind direction dependent offset which is the function of γ. The coefficients $q_1 = 1.415 \times 10^{-6}$, $q_2 = 8.511 \times 10^{-4}$ and $q_3 = 1.007$ were obtained by linear least square regression of $f(\alpha, \gamma)$ versus arccosine of the actual cosine responses for the range of $-70° \leq \alpha \leq 70°$ (van der Molen et al., 2004). For the large angles, $|\alpha| > 70°$, $f(\alpha, \gamma)$ was connected linearly to $f(\pm 90, \gamma)$ at $\alpha = \pm 90°$.

The phase shift of $f_{\mathrm{cr}}(\alpha, \gamma)$ was represented by the offset function $\delta(\gamma)$. From the wind tunnel data, van der Molen et al. (2004) presented $\delta(\gamma)$ as a quadratic function of γ in the wind direction $0° \leq \gamma \leq 60°$, and they regarded $\delta(\gamma)$ for the range of $60° \leq \gamma \leq 120°$ as identical to $\delta(120° - \gamma)$, neglecting the position

of the transducer. However, the phase shift in the wind tunnel data is most likely the result of the underestimation of $a_{\mathrm{cr}}(\alpha, \gamma)$ at positive angles of attack α which can be explained by the transducer shadowing effect (see Kaimal and Finnigan, 1994), and hence the vertical position of the transducer cannot be neglected. In case of $\gamma = 90°$ where the transducer is on the upper side, the shadowing effect may occur at negative α, and hence the phase of $f_{\mathrm{cr}}(\alpha, \gamma)$ may shift to the positive α.

We propose the alternative function $\delta(\gamma)$ which is written as follows:

$$\delta(\gamma) = r \sin(3\gamma), \tag{12}$$

where $r = 6.280$ is a constant obtained by least square regression.

Though there is no experimental proof for the wind direction of $60° \leq \gamma \leq 360°$ (van der Molen et al., 2004), our cosine response function $f_{\mathrm{cr}}(\alpha, \gamma)$ can be supported by several facts.

First, from the "certificate of calibration" in the User Manual of the R3-50, the effect of the frame (strut) on the horizontal windspeed is small ($< \pm 3\%$),which is consistent with the result of van der Molen et al. (2004), who derived the cosine response data with an R2 instrument in calibrated mode. Note that the manufacturer's on-line calibration corrects the horizontal windspeed but does not account for angle of attack errors. The frame may not affect the relationships between the horizontal wind component and the angle of attack α because the frame seems almost homogeneous along the vertical axis. Hence, the effect of the frame on the cosine response function $f_{\mathrm{cr}}(\alpha, \gamma)$ should be negligible.

Second, the cubic function part of Eq. (11), $q_1\alpha^3 + q_2\alpha_2 + q_3\alpha$, is common in the range of $0° \leq \gamma \leq 60°$, which is supported by the wind tunnel data. This part describes the distortion of the cosine response function $f_{\rm cr}(\alpha, \gamma)$. The only difference of the design of Solent ultrasonic anemometer between $0° \leq \gamma \leq 60°$ and $60° \leq \gamma \leq 120°$ is the vertical position of the transducer, and hence the skewness in $60° \leq \gamma \leq 120°$ may be equal to that in $0° \leq \gamma \leq 60°$. Therefore this cubic function part should be applicable for all the wind direction γ.

Third, the phase shift effect of van der Molen et al. (2004) was the result of the underestimation of $a_{\rm cr}(\alpha, \gamma)$ at positive angles of attack α where the wind attacked the lower transducer. This effect is consistent with the fact that the effect of transducer shadowing (velocity attenuation) depends on the angle between the wind vector and the path-way of the transducers, and is the largest when these are identical (see Kaimal and Finnigan, 1994). Therefore the phase shift effect can be regarded as the result of the transducer shadowing (or flow distortion by transducer), and the opposite shift of the phase is expected in the range of $60° \leq \gamma \leq 120°$ where the transducer is on the upper side. Furthermore, the upper and lower transducers appear alternately and regularly at exact intervals of 60°. This fact supports the offset function $\delta(\gamma)$ being a sine function of triple-angle of γ (Eq. (12)).

Figure 4 shows the result of fitting the function for cosine response $f_{\rm cr}(\alpha, \gamma)$ at $\gamma = 0°$ (Fig. 4(a)) and 30° (Fig. 4(b)). The circles indicate the observed cosine response $a_{\rm cr}(\alpha, \gamma)$ averaged for the windspeed of 8 and 16 m s^{-1} and the errorbars show the maximum and minimum values of all the observed $a_{\rm cr}(\alpha, \gamma)$ at each angle of attack α and wind direction γ. The RMSE of $f_{\rm cr}(\alpha, \gamma)$ was 0.0361 which is worse than the case of $f_{\rm sr}(\alpha)$. Nevertheless, Eq. (11) provides a sufficiently good fit.

2.2.3 Calculation

The nonlinear equation which relates α and α' can be derived by substituting Eqs. (7) and (10) into Eq. (5).

$$L(\alpha)\sin\alpha + a_{\mathrm{sr}}(0) - \tan\alpha'\cos\left(f(\alpha,\gamma)\right) = 0 \tag{13}$$

Eq. (13) can be solved uniquely, and α can be estimated from α' (or U, w) analytically.

In solving this equation with the Steffensen method, Eq. (13) must be rewritten as $\alpha = g(\alpha)$. We took the re-arrangement of Eq. (13) shown below which is able to be solved with this method.

$$\alpha = \arctan\frac{\tan\alpha'\cos\left(f(\alpha,\gamma)\right) - a_{\mathrm{sr}}(0)}{L(\alpha)\cos\alpha} \tag{14}$$

The threshold limit $\varepsilon = 0.01$ (deg) was used in the calculation.

2.3 Field data

To evaluate the effect of applying an angle of attack dependent calibration on the actual eddy fluxes of sensible heat H (W m^{-2}), latent heat λE (W m^{-2}) and CO_2 flux F_c (μmol m^{-2} s^{-1}), and on the energy balance closure, the correction method was applied to eddy covariance field data collected at two different forests. One is a birch forest (44° 23′ 03″ N, 142° 19′ 07″ E, 585m ASL) and the other is a mixed forest of evergreen conifers and deciduous broadleaved trees (44° 19′ 19″N, 142° 15′ 41″E, 340m ASL) (Nakai et al., 2005). The birch forest site (hereafter Birch) is located near a mountain ridge, and has an inclination to the west (about 4° near the tower and a maximum

of about 13° on the west side slope). The mixed forest site (hereafter Mixed) also slopes gently to the west (about 3°). Both sites are in Uryu experimental forest, Field Science Center for Northern Biosphere, Hokkaido University, and located in Moshiri, Hokkaido, Japan. Table 2 presents a list of the structure factors of vegetation canopies and measurement heights of eddy covariance systems for the Birch and Mixed forest sites. Though the maximum tree height of the Mixed forest was higher than the measurement height, this highest tree was located downslope and distant from the tower. The tree heights near the Mixed forest flux tower were small enough for the eddy flux instruments to be above the canopy.

At both sites, windspeeds and air temperature were measured with R3-50 Solent ultrasonic anemometers (Gill Instruments, Lymington, UK) in calibrated mode, and concentrations of water vapour and CO_2 were measured with LI-7500 open path infra-red gas analysers (LI-COR, Lincoln, USA). These data were sampled at a rate of 10Hz. Net radiation R_n (W m^{-2}) was also measured with CNR1 (Kipp & Zonen, Delft, Netherlands) radiometers and ground heat flux G (W m^{-2}) with PHF-01 (REBS Inc., Seattle, USA) flux plates.

For comparison, the data from Horstermeer in the Netherlands (52° 15′ N, 5° 5′ E, −2m ASL) was also used: this site is a flat peat bog with a mean vegetation height of about 0.3m (Gash and Dolman, 2003; van der Molen et al., 2004). Table 2 also shows information of this site. For a more detailed description see Gash and Dolman (2003) and van der Molen et al. (2004).

3 Results and discussion

3.1 Reliability of the calculation method

The method proposed here differs from that given by van der Molen et al. (2004) in the numerical scheme and the forms of the (co)sine response functions. Both these methods converge to the same value of the 'true' angle of attack α : for example, with an initial value of $\alpha' = 60°$ with $\gamma = 0°$, both methods gave a final converged value of $\alpha = 62.29°$, by using equations (1) and (2). However, van der Molen et al. (2004) used the value of the second iteration, $\alpha = 62.13°$, which had not reached the convergent value, underestimating by $-0.16°$. The Steffensen method can thus achieve the same accuracy as the van der Molen et al. (2004) method, but with the convergent value being reached in about half the number of iterations. When the threshold limit ε was set as $\varepsilon = 0.01$, the Steffensen method required 2 iterations whereas the method of van der Molen et al. (2004) needed 4 iterations. Applying both methods to flux calculation with $\varepsilon = 0.01$, the increase in computation time over the uncorrected case was 41.5% with method of van der Molen et al. (2004), but 30.2% with our method. Thus our method achieved higher accuracy in less computation time.

3.2 Application to the field data

3.2.1 Instantaneous data

If the observed u, v and w are properly corrected to u_c, v_c and w_c, respectively, then the corrected w_c/V_c is identical to $\sin\alpha$, where $V_c = \sqrt{u_c^2 + v_c^2 + w_c^2}$.

Figure 5 shows the result of correcting for sine response with the method of this study and van der Molen et al. (2004) as the plot of w_c/V_c (Fig. 5(a)) and its difference from $\sin\alpha$, $w_c/V_c - \sin\alpha$ (Fig. 5(b)), against the angle of attack α. The data used here was the instantaneous raw data from 12:20 to 12:25 of 20 August 2003 collected at the Mixed forest site. As expected, the results of w_c/V_c with van der Molen et al. (2004) deviated from $\sin\alpha$ at large angle of attack. Fig. 5 also shows some large deviations in w_c/V_c close to zero. This error is the result of the problem mentioned in Section 1: w_c diverged from Eq. (1) at around $\alpha = -0.64°$, and the resulting absolute value of $\alpha = \arctan(w_c/U_c)$ became large. Hence the converted α deviated near $\alpha = -0.64°$ and there was a gap (Fig. 5). As a result, the RMSE of the corrected w_c/V_c with van der Molen et al. (2004) was 0.0239, whereas it was almost zero (in order of 10^{-6}) with our method.

Following Gash and Dolman (2003), the frequency of occurrence of α was evaluated. Figure 6 shows the results of the frequency of occurrence of α in the Birch and Mixed forest sites at 12:00 – 12:30, 20 August 2003. The averaged windspeed (before correction) of the Birch and Mixed forest sites in this period were 3.61 and 1.98 (m s^{-1}), respectively. The frequency of occurrence of α with van der Molen et al. (2004) is skewed because of the wrong conversion of angles of attack in both the Birch (Fig. 6(a)) and Mixed forest (Fig. 6(b)): the graph of $-5° \leq \alpha \leq 0°$ caved in and the data of this bin moved to other bins of α. The distribution of the frequency of α was spread more widely at large angles of attack in the Mixed forest compared with that in the Birch forest. The roughness length of the Mixed forest was larger than that of the Birch forest (Table 2), and hence this relationship was consistent with the findings of Gash and Dolman (2003).

Figure 7 is the plot of cumulative frequency of angle of attack and sensible heat, latent heat and CO_2 fluxes against the envelope of angle of attack for the Birch (Fig. 7(a)) and Mixed forest (Fig. 7(b)) calculated with our method. Cumulative frequency of the eddy fluxes were calculated from the flux-angle distribution function (Gash and Dolman, 2003). In the Birch forest, 16.1% of the samples had eddies with angles outside the manufacturer's specified envelope of $\pm 20°$, and these carried 45.0, 45.2 and 44.0% of the sensible heat, latent heat and CO_2 fluxes respectively. For the Mixed forest, 45.7% of the samples corresponded to 'out of spec' angles, and these angles accounted for 79.6, 74.5 and 74.3% of the sensible heat, latent heat and CO_2 fluxes respectively. Gash and Dolman (2003) showed that in Horstermeer peat bog, only 3% of the samples had angles outside the limit and they carried 18, 20, 20 and 8% of the sensible heat, latent heat, and negative and positive CO_2 fluxes, respectively. These results emphasise that the angle of attack dependent errors of ultrasonic anemometer cannot be neglected, especially over the rough forest.

3.2.2 Eddy covariance

Here we discuss the effect of (co)sine error correction on the actual eddy fluxes of sensible heat (H), latent heat (λE) and CO_2 (F_c), and on the energy balance closure. Eddy fluxes were calculated for each half-hour run using linear time averaging and the following procedure:

(1) Humidity correction of sonic temperature (Schotanus et al., 1983)

(2) Correction of angle of attack dependent error

(3) Coordinate rotation for $\overline{v} = 0$, $\overline{w} = 0$ (McMillen, 1988; Kaimal and

Finnigan, 1994)

(4) Frequency response corrections (Moore, 1986)

(5) WPL correction (Webb et al., 1980)

Crosswind correction of sonic temperature (Schotanus et al., 1983; Kaimal and Gaynor, 1991) was already applied in the on-board software of R3-50.

The Birch and Mixed forest data were used from September 2003. To remove obviously erroneous results, λE and F_c were filtered using the standard deviation of water vapour concentration q (kg m^{-3}), σ_q, and CO_2 concentration c (kg m^{-3}), σ_c, respectively. The threshold values used here were $\sigma_q = 10^{-3}$ (kg m^{-3}) and $\sigma_c = 10^{-5}$ (kg m^{-3}).

There were linear relationships between uncorrected and corrected fluxes, and hence the effect of correction on the eddy fluxes can be found by linear regression through origin. Table 3 compares the effect of (co)sine error correction on the output of H, λE and F_c. After applying the method of correction proposed here, all the fluxes were found to increase. In the Birch forest, H, λE and F_c were increased by 9.0%, 6.9% and 6.7%, respectively, and similarly by 13.2%, 10.5% and 9.9% in the Mixed forest. The increments with the van der Molen et al. (2004) were smaller than those with our method for all the fluxes. The differences between our method and van der Molen et al. (2004) were 2.5 – 2.8% in the Birch and 2.3 – 3.1% in the Mixed forest. As mentioned in Section 3.1, the method of van der Molen et al. (2004) slightly underestimates α as a result of the incomplete conversion, which might be a cause of underestimation in correcting eddy fluxes.

On the other hand, for the data from short vegetation in Horstermeer (3 May – 2 July 2002), our method increased H, λE and F_c by 5.0%, 4.8% and 2.7%,

respectively, and the difference between our method and van der Molen et al. (2004) were 0.3 – 1.2% (Table 3). These results were smaller than those of the Birch and Mixed forest, indicating that the (co)sine error was worse over rough forest than short vegetation, and that the effect of the correction was large over the rougher vegetation. Nevertheless the effect cannot be neglected even for this short vegetation.

As H and λE were increased by the (co)sine error correction, the energy balance closure is expected to be improved. Figure 8 shows the scatter diagram of $H+\lambda E$ against available energy R_n-G in the Birch (a) and Mixed forest (b). The results with and without correction by our method are shown, together with regression lines forced through the origin. Although the data vary widely, the regression lines show a clear increase in slope when the angle of attack correction is included. Table 4 gives the energy balance closure rate in both sites, comparing the different (co)sine error correction methods. Using our method, the closure rates improved at both sites by correcting the angle of attack error: from 86.8% to 93.7% in the Birch, and from 91.0% to 101.7% in the Mixed forest. Our method also improved the closure rates by 2.4% for both the Birch and Mixed forest compared with the results of van der Molen et al. (2004).

Estimating the energy balance at Horstermeer is problematic because, being true wetland, a significant proportion of the energy is absorbed by the water at, or close to, the surface. This water is not stagnant but is thought to flow slowly through the bog. However, although the energy going into the water is unknown, the closure rate of $H + \lambda E$ against R_n was increased from 72.0% to 74.8% by our method (Table 4). The increment of the rate in Horstermeer was small (2.8%) compared with that in the Birch (6.5%) and Mixed forest

(10.4%), indicating that, as would be expected from the analysis of Gash and Dolman (2003), the effect of (co)sine error correction on the energy balance closure was larger over the rough forest than that over the short vegetation.

The original concept of correcting for angle of attack error by applying an angle-dependent calibration (Gash and Dolman, 2003; van der Molen et al., 2004) has contributed to the improvement of the energy balance closure. The method proposed here gives a more robust and efficient procedure with extra improvement of the closure.

4 Conclusions

This study introduces an improved method of correcting the angle of attack dependent errors of ultrasonic anemometers. The proposed method is more rigorous in that it derives the 'true' angle of attack by solving the nonlinear equation connecting it to the observed U and w. This equation can be solved by using the Steffensen method. The method is robust and adequately fast for practical use in calculating eddy fluxes.

In applying the method to R2- and R3-type Solent ultrasonic anemometers, the function fitted to the observed sine response was improved by using a logistic regression, which removed the disadvantages of the previous method of van der Molen et al. (2004) achieving continuity at $\alpha = 0°$ and a better fit at extreme angles. Moreover, the cosine response function was also improved to consider the effect of the flip in the vertical position of the transducers.

The method proposed here provides the following improvements over the method of van der Molen et al. (2004).

- Higher accuracy in less computation time
- Removal of the deviation at large angles of attack α and wrong conversion of α near $\alpha = -0.64°$
- Inclusion of the effect of the vertical positions of the transducers on the cosine response

Applying our method to field data from two forest sites and one short vegetation site, eddy fluxes were increased by 6.7 – 9.0% in the Birch, 9.9 – 13.2% in the Mixed forest and 2.7 – 5.0% in Horstermeer peat bog. These results were 0.3 – 3.1% larger than those found using the method of van der Molen et al. (2004). As a result, the energy balance closure rates were significantly improved with our correction method in these sites. These results indicate that a large portion of the energy imbalance can be accounted for by the ultrasonic anemometer angle of attack dependent errors.

It is recommended that other ultrasonic anemometers are checked for angle of attack errors in wind tunnel experiments, and calibration functions are derived. Our method can be applied equally well to any other functions, but note that the discontinuity of the function may cause a computation error or endless loop in the calculation.

Acknowledgement

Authors would like to thank Dr. Kyoko Kato of JST/CREST researcher in Hokkaido University who supplied the forest structure data for the experimental sites, and the staff of Uryu Experimental Forest, Hokkaido University.

A The analytical solution of nonlinear equation with Steffensen method

Here we note the method to solve the nonlinear equation $x = g(x)$ with the Steffensen method. The basis of this method is linear iteration which calculates the following equation iteratively for successive approximation

$$x_{i+1} = g(x_i). \tag{A.1}$$

The subscript $i(= 1, 2, ...)$ indicates the number of iteration. When the initial value x_0 is obtained, then $x_1 = g(x_0)$ and $x_2 = g(x_1)$. The Steffensen method calculates the following approximate value x_3 as follows

$$x_3 = x_0 - \frac{(x_1 - x_0)^2}{x_2 - 2x_1 + x_0}. \tag{A.2}$$

This x_3 is used as the initial value x_0 for the next calculation iteratively, until x converges to the solution.

The computational procedure is written as follows.

(1) Apply the initial value x_0, and set the threshold limit ε.

(2) $x_1 = g(x_0)$

(3) $x_2 = g(x_1)$

(4) $x_3 = x_2$

(5) If $|x_2 - 2x_1 + x_0| < \varepsilon$ then go to (8).

(6) $x_3 = x_0 - \dfrac{(x_1 - x_0)^2}{x_2 - 2x_1 + x_0}$

(7) Put $x_0 = x_3$ and go back to (2).

(8) Return the solution $x = x_3$.

B Step-by-step correction procedure

The actual correction procedure proposed in this study may be summarised as follows.

(1) Using the individual raw data samples of u, v and w, calculate the first estimate of the angle of attack

$$\alpha' = \frac{w}{\sqrt{u^2 + v^2}}$$

and the horizontal wind direction γ.

(2) Solve the non-linear Steffensen method, as described in Appendix A, to derive the 'true' angle of attack as follows:

(a) Use α_0 as the initial angle of attack α': $\alpha_0 = \alpha'$

(b) Apply α_0 in:

$$\alpha_1 = g(\alpha_0) = \arctan \frac{\tan \alpha' \cos \{f(\alpha_0, \gamma)\} - a_{\mathrm{sr}}(0)}{L(\alpha_0) \cos \alpha_0}$$

to obtain α_1, where $L(\alpha)$ is given by the Eqs. (8) and (9), $f(\alpha, \gamma)$ by Eq. (11) and $a_{\mathrm{sr}}(0) = 0.0195$.

(c) In a similar way, apply α_1 in

$$\alpha_2 = g(\alpha_1) = \arctan \frac{\tan \alpha' \cos \{f(\alpha_1, \gamma)\} - a_{\mathrm{sr}}(0)}{L(\alpha_1) \cos \alpha_1}$$

to obtain α_2.

(d) Set α_3 equal to α_2: $\alpha_3 = \alpha_2$

(e) Goto (h) if $|\alpha_2 - 2\alpha_1 + \alpha_0| < \varepsilon$, the resolved 'true' angle of attack is α_3. Choose $\varepsilon = 0.01$.

(f) If the calculation has not yet converged, proceed with:

$$\alpha_3 = \alpha_0 - \frac{(\alpha_1 - \alpha_0)^2}{\alpha_2 - 2\alpha_1 + \alpha_0}$$

(g) Now replace the initial value α_0 by the value of α_3 obtained in (f) and go back to (b), until breaking out of the loop in (e).

(h) This point will only be reached if the angle of attack has converged sufficiently. This has resulted in a 'true' angle of attack α_3.

(3) Calculate the corrected horizontal wind speed components u_c and v_c as:

$$u_c = u\frac{\cos\alpha}{f_{\rm cr}(\alpha,\gamma)}, \quad v_c = v\frac{\cos\alpha}{f_{\rm cr}(\alpha,\gamma)}$$

(4) Calculate the corrected vertical wind speed component w_c as:

$$w_c = \sqrt{u_c^2 + v_c^2}\tan\alpha \quad or \quad w_c = w\frac{\sin\alpha}{f_{\rm sr}(\alpha)} \text{ (when } \alpha = \pm 90^\circ)$$

This process must be applied to each individual raw measurement of u, v and w before any other calculation or correction procedure used in calculating eddy fluxes.

C Subroutine for angle of attack error correction

The source code of a subroutine for correcting ultrasonic anemometer angle of attack errors is available in several programming languages (C/C++, FORTRAN, MATLAB, BASIC). These can be downloaded from the following websites.

- Website of Taro Nakai (http://todomatsu.lowtem.hokudai.ac.jp/~taro/)
- Website of M.K. van der Molen (http://www.geo.vu.nl/~moli/)
- CREST/WECNoF website (http://www.agr.nagoya-u.ac.jp/~wecnof/)

Note that the subroutine is designed for R2- and R3-type Solent ultrasonic anemometers (Gill Instruments, Lymington, UK). Hence is applicable only for following anemometers that have an identical shape.

- Solent WindMaster
- Solent WindMaster Pro
- Solent R2
- Solent R3
- Solent R3-50

For other models the functions $f_{\mathrm{sr}}(\alpha)$ and $f_{\mathrm{cr}}(\alpha, \gamma)$ need to be replaced with functions fitted to appropriate wind tunnel data.

References

Burden, R.L., Faires, J.D., 2004. Numerical Analysis, 8th ed., Brooks/Cole, Pacific Grove, CA, 850pp.

Conway, G.R., Glass, N.R., Wilcox, J.C., 1970. Fitting nonlinear models to biological data by Marquardt's algorithm. Ecology 51, 503–507.

Farnum, N.R. 1991. A fixed point method for finding percentage points. Appl. Statist. 40, 123–126.

Gash, J.H.C., Dolman, A.J., 2003. Sonic anemometer (co)sine response and flux measurement. I. The potential for (co)sine error to affect sonic anemometer-based flux measurements. Agric. For. Meteorol. 119, 195–207.

Johnson, L.W., Scholz, D.R., 1968. On Steffensen's method. SIAM J. Numer. Anal. 5, 296–302.

Kaimal, J.C., Gaynor, J.E., 1991. Another look at sonic thermometry. Boundary Layer Meteorol. 56, 401–410.

Kaimal, J.C., Finnigan, J.J., 1994. Boundary Layer Flows. Oxford University Press, Oxford, 289 pp.

McMillen, R.T., 1988. An eddy correlation technique with extended applica-

bility to non-simple terrain. Boundary Layer Meteorol. 43, 231–245.

Moore, C.J., 1986. Frequency response corrections for eddy correlation systems. Boundary-Layer Meteorol. 37, 17–35.

Nakai, T., Kuwada, T., Kodama, Y., Ohta, T., Maximov, T.C., 2005. Comparison of aerodynamic characteristics among boreal, cool-temperate and warm-temperate forests. J. Agric. Meteorol., 60(5), 689–692.

Schotanus, P., Nieuwstadt, F.T.M., DeBruin, H.A.R., 1983. Temperature measurement with a sonic anemometer and its application to heat and moisture fluctuations. Boundary Layer Meteorol. 26, 81–93.

van der Molen, M.K., Gash, J.H.C., Elbers, J.A., 2004. Sonic anemometer (co)sine response and flux measurement. II. The effect of introducing an angle of attack dependent calibration. Agric. For. Meteorol. 122, 95–109.

Webb, E.K., Pearman, G.I., Leuning, R., 1980. Correction of flux measurements for density effects due to heat and water vapour transfer. Q. J. R. Meteorol. Soc. 106, 85–100.

Wilson, K., Goldstein, A., Falge, E., Aubinet, M., Baldocchi, D., Berbigier, P., Bernhofer, C., Ceulemans, R., Dolman, A., Field, C., Grelle, A., Ibrom, A., Law, B.E., Kowlaski, A., Meyers, T., Moncrieff, M., Monson, R., Oechel, W., Tenhunen, J., Valentini, R., Verma, S., 2002. Energy balance closure at FLUXNET sites. Agric. For. Meteorol. 113, 223–243.

Table 1: The coefficients in equations (8) and (9)

	p_1	p_2	p_3	p_4
$-90 \leq \alpha < 0$	0.429	55.59	0.223	0.488
$0 \leq \alpha \leq 90$	0.571	1610.9	0.111	0.972

Table 2: The list of the structure factors of vegetation canopies and measurement heights of eddy covariance systems about the Birch forest, Mixed forest and Horstermeer peat bog sites.

	Birch forest	Mixed forest	Horstermeer
Stand density (stands ha^{-1})	4,384	2,585	—
Mean vegetation height (m)	10.6	5.3	0.3 (typical)
Maximum vegetation height (m)	13.8	35.5	1.0
Roughness length (m)	0.53*	2.08*	0.03
Zero-plane displacement (m)	10.2*	18.8*	0.2
Measurement height (m)	21.1	31.6	4.7

*Estimated for September 2003.

Table 3: The effect of (co)sine error correction on the output of energy and CO_2 fluxes in the Birch and Mixed forest (September 2003) and Horstermeer peat bog (3 May – 2 July 2002).

	Birch forest			Mixed forest			Horstermeer peat bog		
Method	H	λE	F_c	H	λE	F_c	H	λE	F_c
Uncorrected	1.000	1.000	1.000	1.000	1.000	1.000	1.000	1.000	1.000
van der Molen et al.(2004)	1.065	1.041	1.040	1.101	1.078	1.076	1.043	1.036	1.024
This study	1.090	1.069	1.067	1.132	1.105	1.099	1.050	1.048	1.027

Table 4: Comparison of energy balance closure rate for different (co)sine error correction methods in Birch and Mixed forest (September 2003) and Horstermeer peat bog (3 May – 2 July 2002).

Method	Birch forest[*1]	Mixed forest[*1]	Horstermeer[*2]
Uncorrected	86.8%	91.0%	72.0%
van der Molen et al.(2004)	91.3%	99.3%	74.7%
This study	93.7%	101.7%	74.8%

[*1] The rate of $H + \lambda E$ against $R_n - G$.

[*2] The rate of $H + \lambda E$ against R_n.

- Fig. 1. Schematic diagram of observed and corrected wind vectors and angles of attack.

- Fig. 2. Distribution of the observed $(a_{\rm sr}(\alpha) - a_{\rm sr}(0))/\sin\alpha$ against α and the logistic function $L(\alpha)$. The circles indicate the averaged data derived from 8 and 16 m s^{-1} tunnel windspeed, and the open and closed triangles indicate 8 and 16 m s^{-1} wind tunnel data, respectively.

- Fig. 3. Behaviour of the new function for sine response compared with the data of the wind tunnel experiments. The circles indicate the averaged data for the wind speed of 8 and 16 m s^{-1}, and the errorbars show the maximum and minimum values of all the experimental data.

- Fig. 4. Behaviour of the function for cosine response $f_{\rm cr}(\alpha, \gamma)$ at (a) $\gamma = 0°$ and (b) $\gamma = 30°$ compared with the data from the wind tunnel experiment. The circles indicate the observed cosine response $a_{\rm cr}(\alpha, \gamma)$ averaged for the windspeed of 8 and 16 m s^{-1} and the errorbars show the maximum and minimum values of all the observed $a_{\rm cr}(\alpha, \gamma)$ at each angle of attack α and wind direction γ.

- Fig. 5. Results of the correction of the sine response with the method of this study and van der Molen et al.(2004): (a) corrected w_c/V_c together with $\sin\alpha$, and (b) the difference of w_c/V_c from $\sin\alpha$. Instantaneous raw data were used (Mixed forest, 12:20 – 12:25, 20 August 2003).

- Fig. 6. Frequency of occurrence of α in (a) the Birch forest and (b) the Mixed forest at 12:00–12:30, 20 August 2003.

- Fig. 7. Cumulative frequency of angle of attack, sensible heat, latent heat

and CO_2 fluxes against the envelope of angle of attack for (a) the Birch forest and (b) the Mixed forest.

- Fig. 8. Energy balance closure between $(R_n - G)$ and $(H + \lambda E)$ in (a) the Birch forest and (b) the Mixed forest sites.

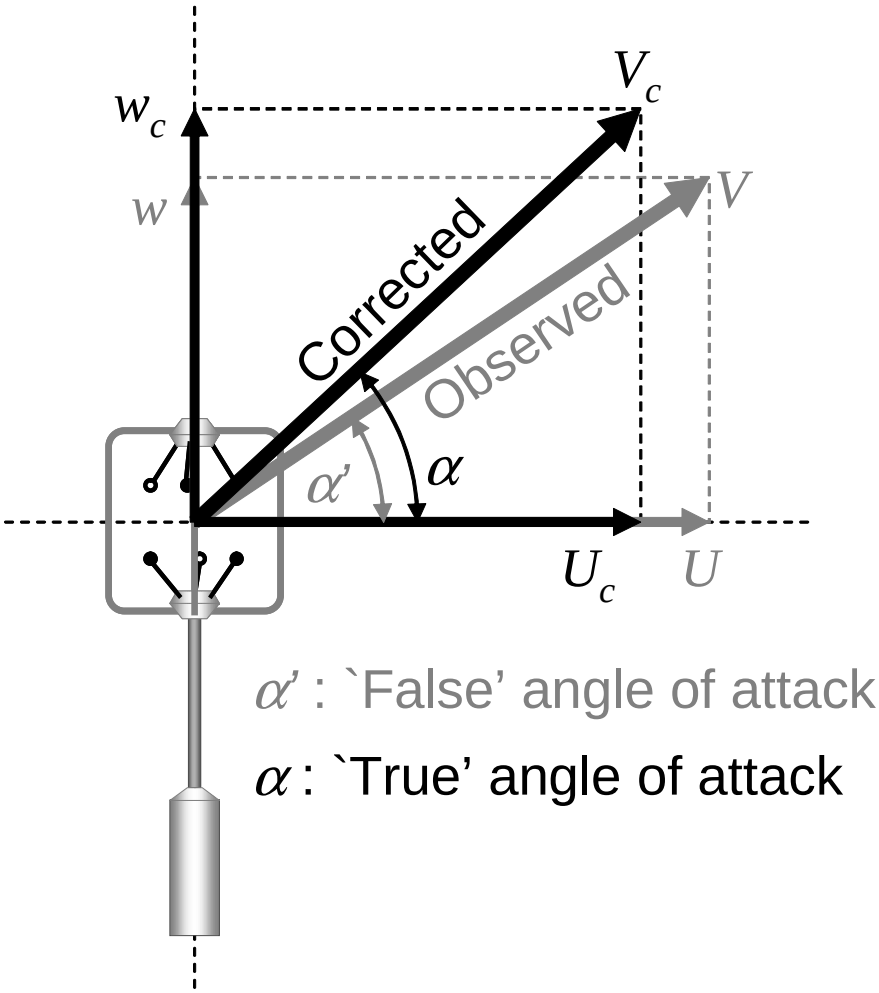
V_c
w_c
w
V
Corrected
Observed
α'
α
U_c
U
α' : `False' angle of attack
α : `True' angle of attack

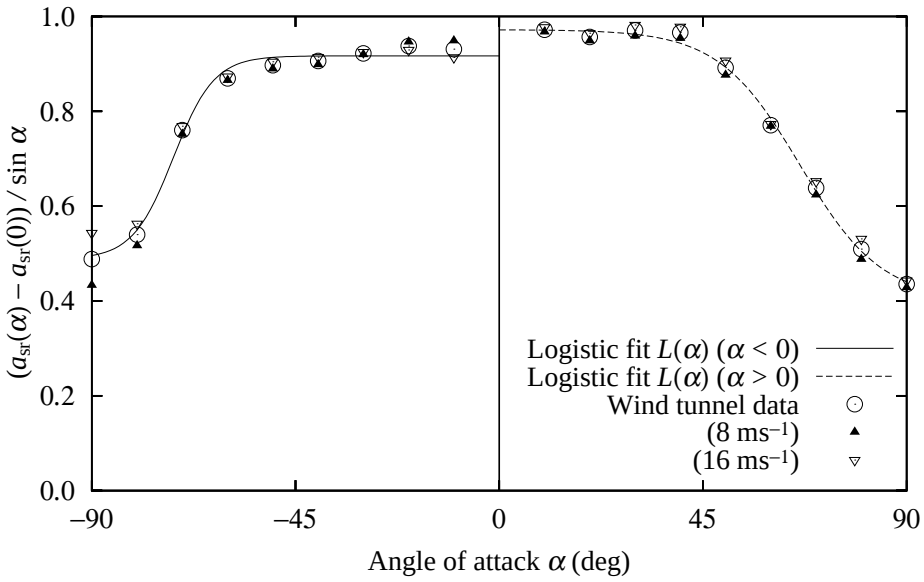
1.0
0.8
0.6
0.4
0.2
0.0
–90
–45
0
45
90
$(a_{sr}(\alpha) - a_{sr}(0)) / \sin\alpha$
Angle of attack α (deg)
Logistic fit $L(\alpha)$ ($\alpha < 0$)
Logistic fit $L(\alpha)$ ($\alpha > 0$)
Wind tunnel data
(8 ms^{-1})
(16 ms^{-1})

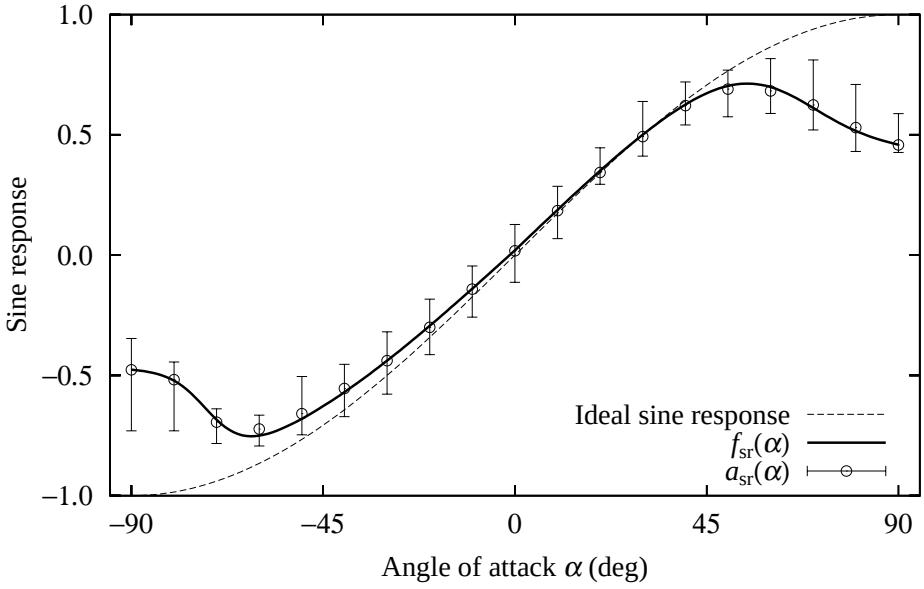
1.0
0.5
0.0
−0.5
−1.0
Sine response
−90
−45
0
45
90
Angle of attack α (deg)
Ideal sine response
$f_{sr}(\alpha)$
$a_{sr}(\alpha)$

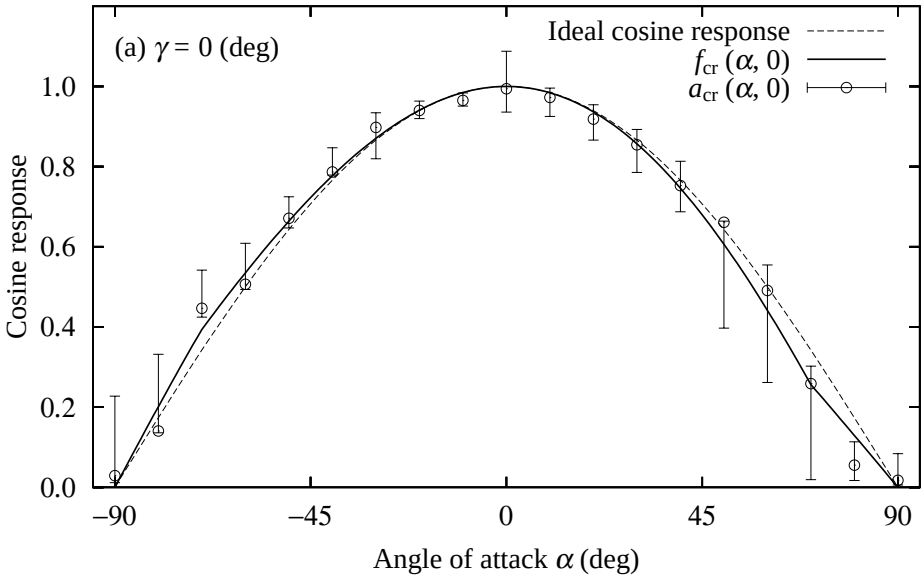
(a) γ = 0 (deg)
Ideal cosine response
f_{cr} (α, 0)
a_{cr} (α, 0)
Cosine response
1.0
0.8
0.6
0.4
0.2
0.0
–90
–45
0
45
90
Angle of attack α (deg)

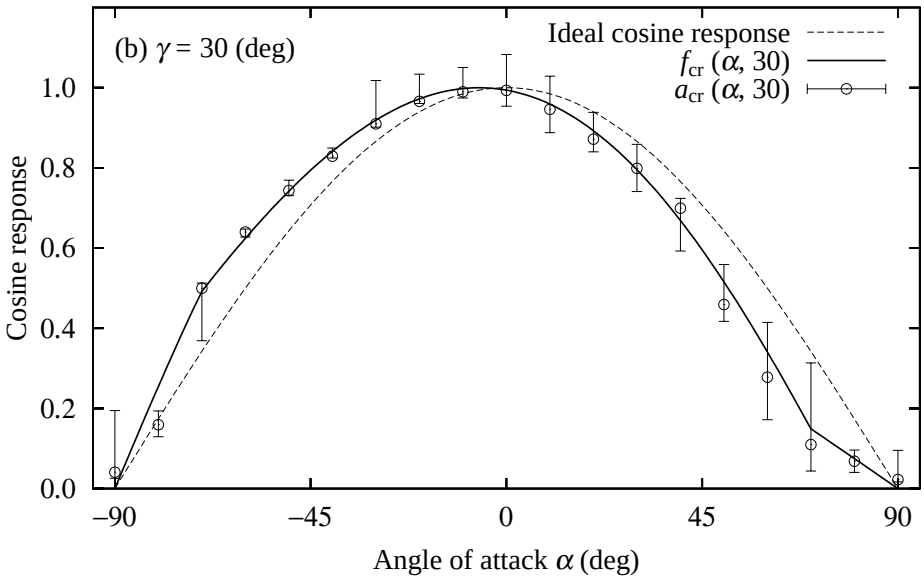
(b) γ = 30 (deg)
Ideal cosine response
f_{cr} (α, 30)
a_{cr} (α, 30)
Cosine response
1.0
0.8
0.6
0.4
0.2
0.0
–90
–45
0
45
90
Angle of attack α (deg)

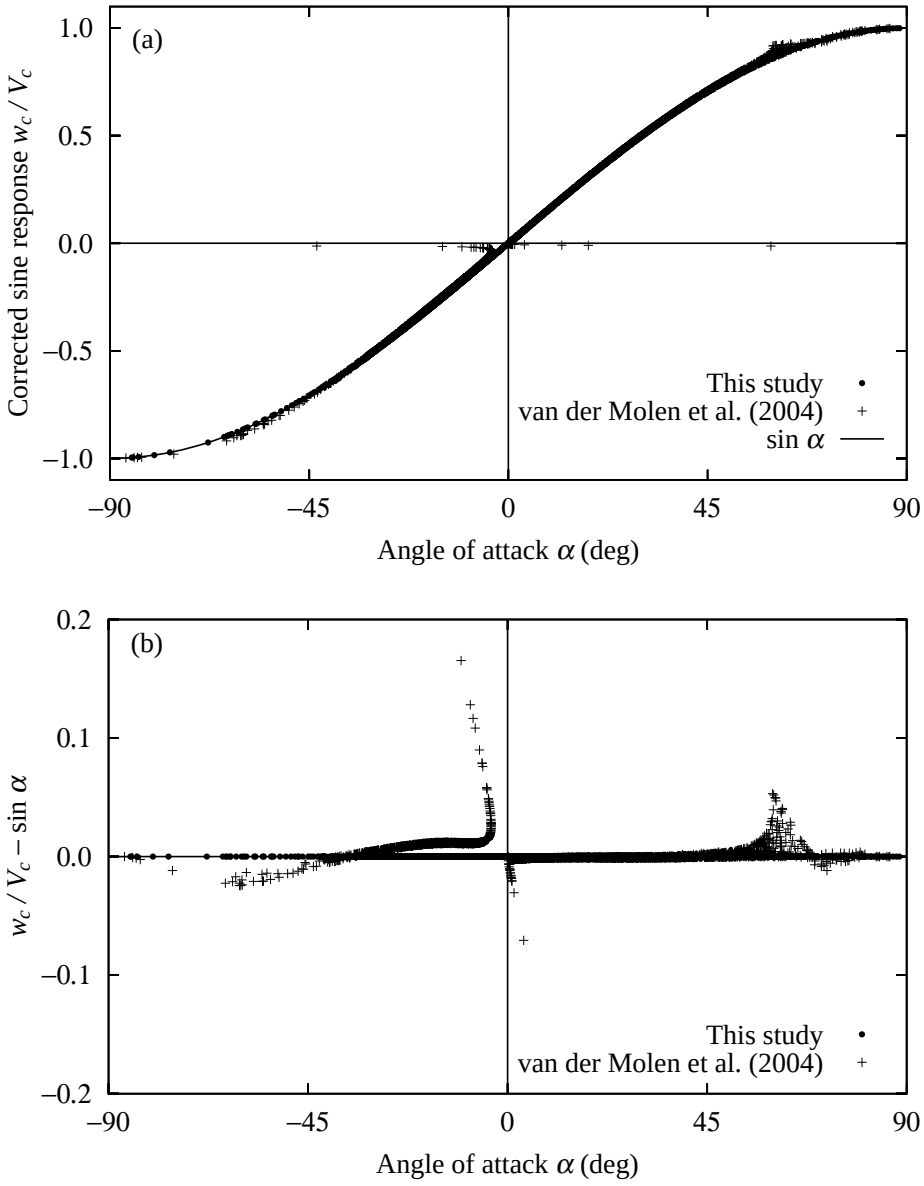
(a)
Corrected sine response w_c / V_c
1.0
0.5
0.0
–0.5
–1.0
This study
van der Molen et al. (2004)
sin α
–90
–45
0
45
90
Angle of attack α (deg)
(b)
w_c / V_c – sin α
0.2
0.1
0.0
–0.1
–0.2
This study
van der Molen et al. (2004)
–90
–45
0
45
90
Angle of attack α (deg)

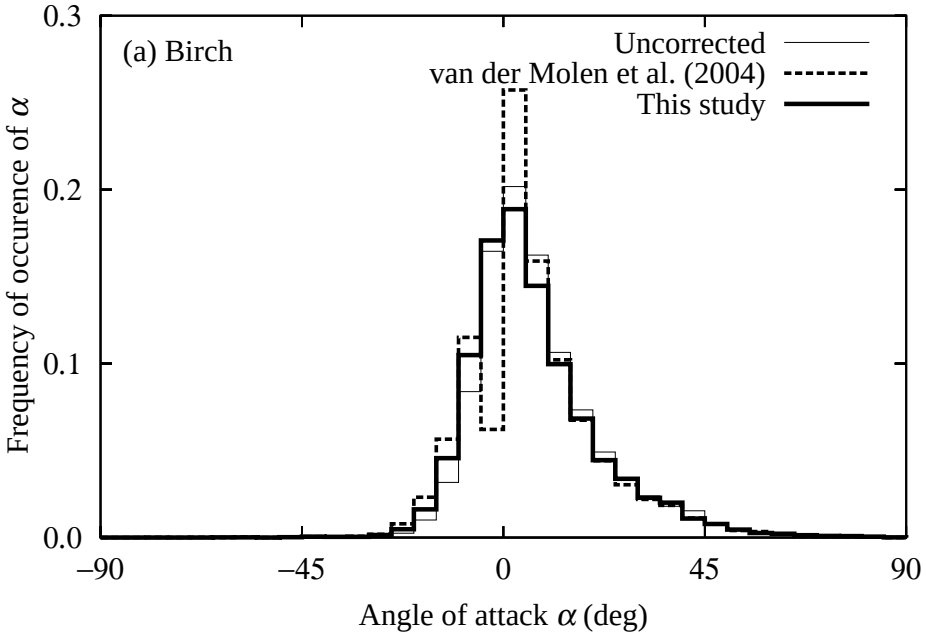
(a) Birch
Uncorrected
van der Molen et al. (2004)
This study
Frequency of occurence of α
Angle of attack α (deg)
0.3
0.2
0.1
0.0
–90
–45
0
45
90

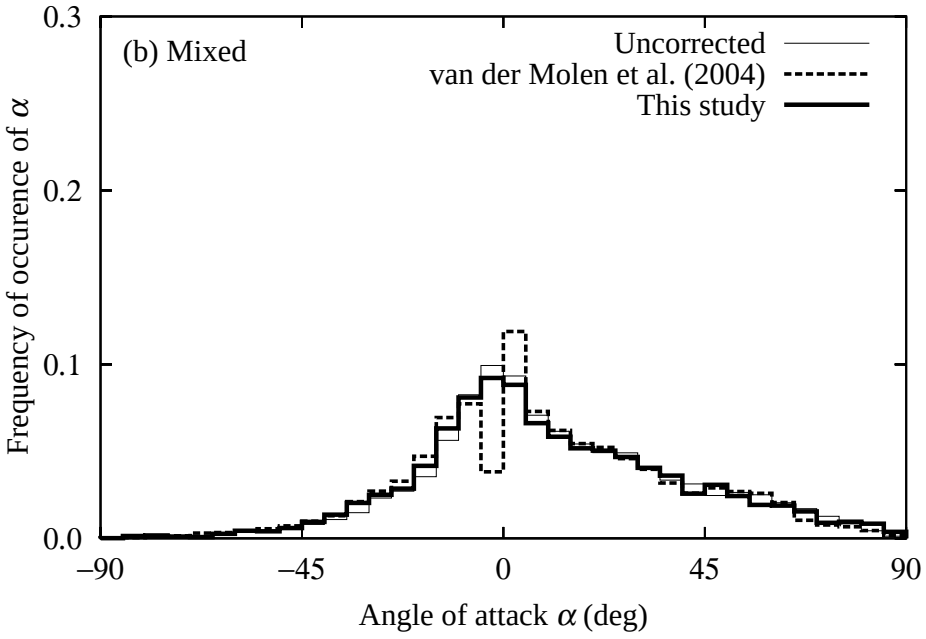
(b) Mixed
Uncorrected
van der Molen et al. (2004)
This study
Frequency of occurence of α
Angle of attack α (deg)
0.3
0.2
0.1
0.0
–90
–45
0
45
90

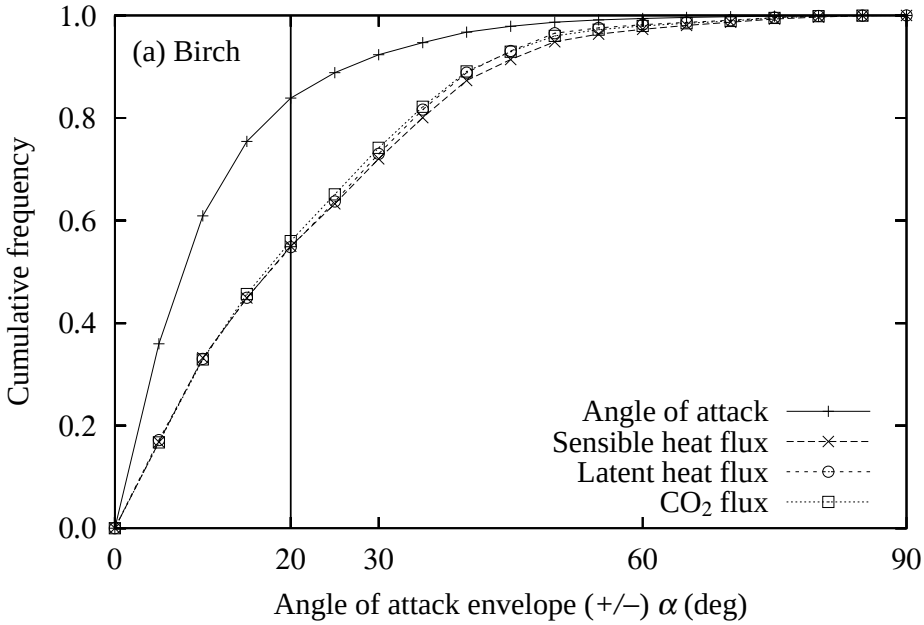
(a) Birch
Cumulative frequency
1.0
0.8
0.6
0.4
0.2
0.0
0
20
30
60
90
Angle of attack envelope (+/–) α (deg)
Angle of attack
Sensible heat flux
Latent heat flux
CO2 flux

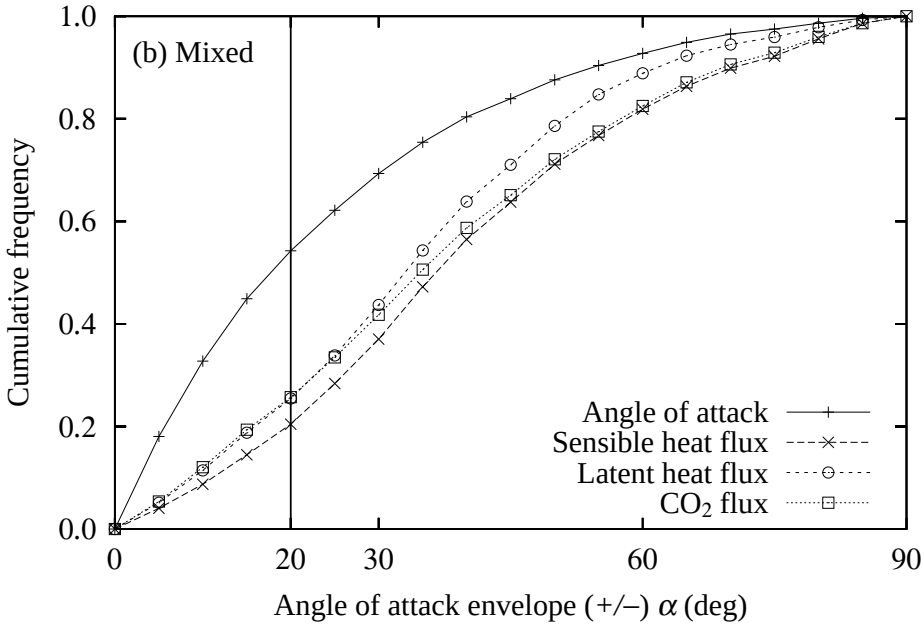
(b) Mixed
Cumulative frequency
1.0
0.8
0.6
0.4
0.2
0.0
0
20
30
60
90
Angle of attack envelope (+/–) α (deg)
Angle of attack
Sensible heat flux
Latent heat flux
CO2 flux

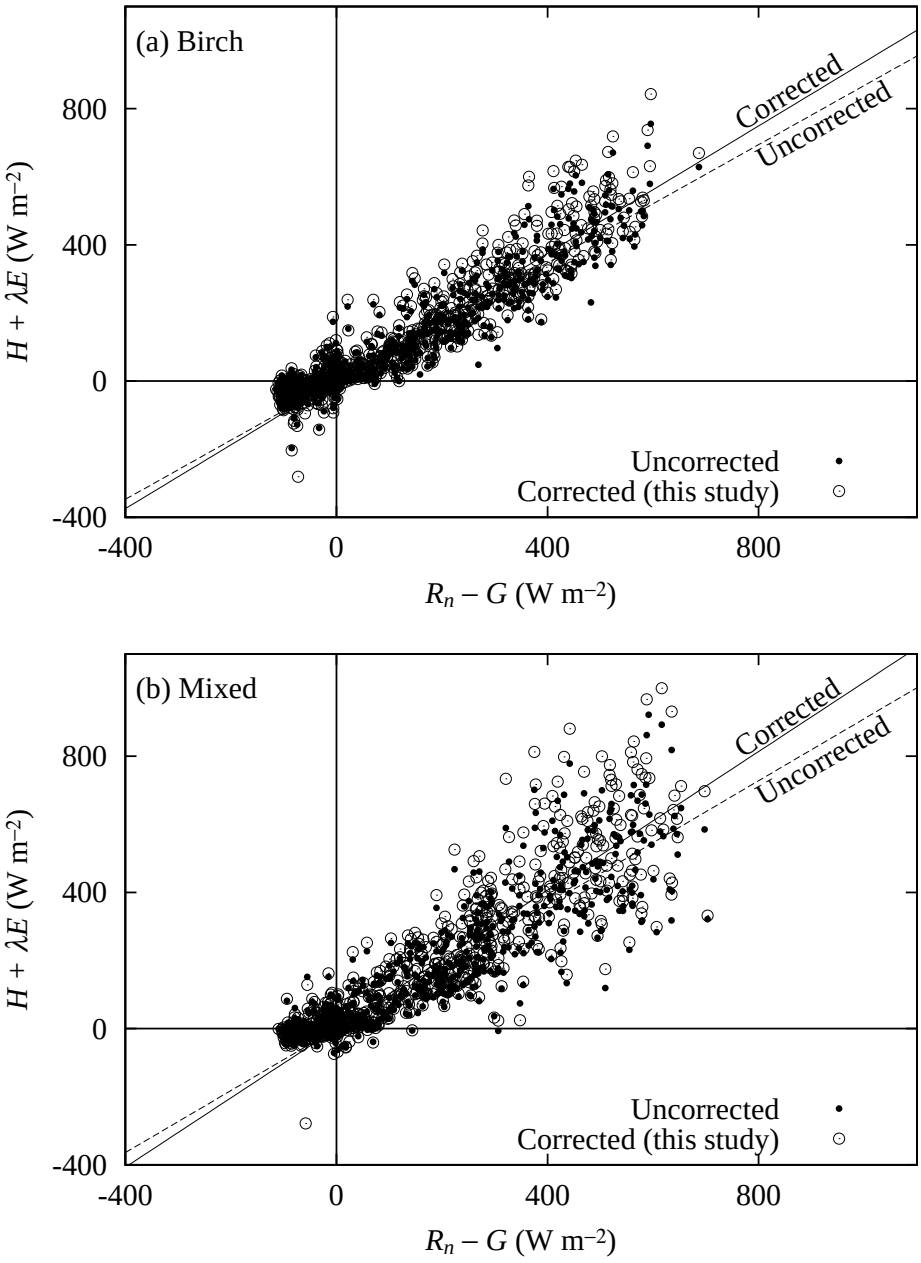
(a) Birch
Corrected
Uncorrected
Uncorrected
Corrected (this study)
800
400
0
-400
-400
0
400
800
$H + \lambda E$ (W m^{-2})
$R_n - G$ (W m^{-2})
(b) Mixed
Corrected
Uncorrected
Uncorrected
Corrected (this study)
800
400
0
-400
-400
0
400
800
$H + \lambda E$ (W m^{-2})
$R_n - G$ (W m^{-2})